

# Reaction Force Analysis of Puncture Robot for CT-guided Interventional Radiology in Animal Experiment

Kohei Sugiyama, Takayuki Matsuno, Tetsushi Kamegawa, Takao Hiraki,  
Hirotaka Nakaya, Akira Yanou and Mamoru Minami

**Abstract**—A medical procedure called Interventional Radiology (IR) is paid much attention in recent years. IR can be performed percutaneously while a doctor observes patient's fluoroscopic image. It has advantage that invasiveness is low compared with conventional surgery. In order to take patient's fluoroscopic image, computed tomography (CT) equipment is often used. In this case, it is problem that the doctor is exposed to radiation because the doctor should conduct the procedure close to CT equipment. Thus, we have developed a robot called "Zerobot" which has six DOF and remote-control feature with dedicated input device. In this paper, first, overview of Robotic IR is described. Then, we describes about animal puncture experiment of Zerobot, and discuss the result of puncture reaction force analysis in the experiment.

## I. INTRODUCTION

There is a surgical method called Interventional Radiology (IR) [1]. This surgical method is conducted with imaging modality such as CT and X-rays. With observing medical images, the surgeon conducts IR treatment percutaneously with inserting a needle or a catheter to the patient body. In particular, CT equipment has high visibility and objectivity. And CT fluoroscopy system, which can show medical images in real time, is superior as guiding tool for IR. So CT-guided IR is applied to lung cancer treatment, liver cancer treatment, biopsy, and so on[2]. The situation of actual procedure is shown in Fig. 1. As compared with conventional survey, IR can be conducted in local anesthesia and this surgical method is minimally-invasive to patients. Moreover patients can be discharged from the hospital about three or four days after treatment. Because of these advantages, IR is paid much attention in recent years. Now IR is conducted by surgeons using a forceps and a needle. The size of malignancy is about 3[mm] in diameter[3]. Therefore operator must puncture a needle carefully and accurately. Because operators conduct procedure close to the CT gantry, operators are exposure to radiation during CT scanning. In order to prevent radiation exposure, operators wear radiation protection aprons and handle a needle using a forceps. However, it is impossible



Fig. 1. Interventional Radiology

to prevent radiation exposure completely. Then some medical robots are developed in order to improve accuracy of positioning of a needle, and to reduce radiation exposure, such as AcuBot[4], CT-Bot[5], and B-Rob[6]. These robots aim to support operators to insert a needle as CT-guided puncture. However, Zerobot, which is developed by us, aims to conduct whole process (from positioning robot to inserting a needle) by remote-control. In this research, Zerobot for clinical assessment has been developed already, and animal experiment using rabbit has been performed.

Concept of Robotic IR is shown in Fig. 2. This paper presents overview of Robotic IR and result of animal experiment. In section II, overview which includes the mechanism of Zerobot, procedure of puncture, input device and system structure is described. The result of animal experiment used Zerobot which is developed is described in section III. Finally, conclusion is provided in section IV.

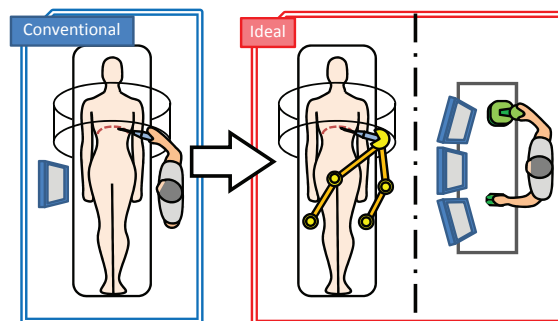


Fig. 2. Concept of Robotic IVR

This work was supported by MEXT KAKENHI Grant Number 13233919 and Research on Development of New Medical Devices 15652923 from Japan Agency for Medical Research and Development, AMED.

K.Sugiyama is with the Graduate School of Natural Science and Technology, Okayama University, Okayama, Japan en422839@s.okayama-u.ac.jp

T.Matsuno, T.Kamegawa, H.Nakaya, A.Yanou and M.Minami are with the Graduate School of Natural Science and Technology, Okayama University, Okayama, Japan

T.Hiraki is with the Department of Radiology, Okayama University Hospital

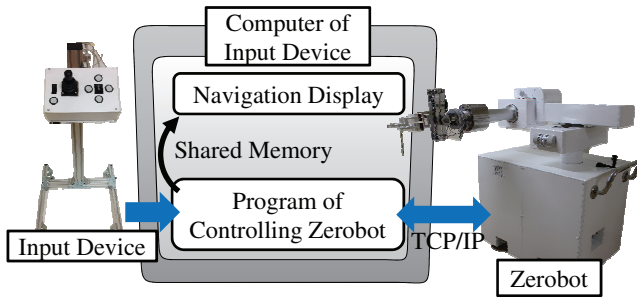


Fig. 3. System Structure of Robotic IR

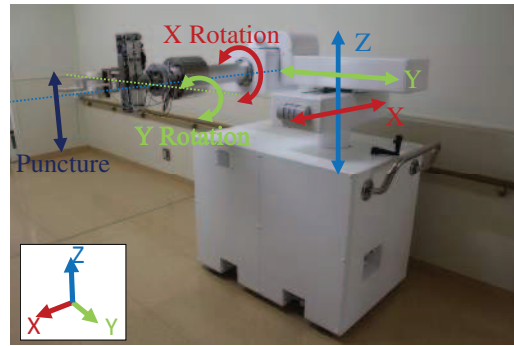


Fig. 4. ZeroBot

## II. OVERVIEW OF ROBOTIC IVR

### A. System Structure

This subsection shows the system structure of Robotic IR. Overview of the structure is shown in Fig. 3. ZeroBot is connected to computer of input device by ethernet to communicate by TCP/IP. As receive the information of status of input device, computer of input device instructs to ZeroBot to actuate axes. ZeroBot sends the values of all actuators and force sensor to input device. In the input device, program of controlling ZeroBot and navigation display is divided, and status of ZeroBot received by program of controlling ZeroBot is sent by shared memory to program of navigation display. Therefore, even if the program of navigation display was stopped caused by some troubles, program of controlling ZeroBot is not affected.

### B. Mechanism

The appearance of ZeroBot is shown in Fig. 4. It has five DOF for needle tip position and needle orientation, and has one DOF in puncturing direction. Six actuators are in the machine. Four linear actuators (X, Y, Z and puncturing axes directions) and two rotational actuators (around the X and Y axes) are included. Therefore, ZeroBot can perform puncture operation by actuating the puncturing axis, regardless of the posture. Four wheels are mounted on the bottom plate of the robot, so it can be moved with human power. At the surgical operation, the robot is located under a bed and fixed by locking the wheels. Changing needle orientation and puncturing are performed in CT-gantry by arm part above patient.

Because of structure of CT equipments, if metal part was in the gantry, incorrect image called artifact will appear on CT image. If artifact appeared, patient's internal image will be obscured and trouble will occur on an surgical operation. Therefore, metal parts cannot be used on needle gripper. Accordingly parts are made of engineering plastic. In addition, puncturing motor and changing orientation motor is detached from CT radiography plane by adopting parallel link mechanism at end-effector, as shown in Fig. 5. Front of a part of gripping needle made of engineering plastic, two force sensors is located. These sensors can measure the moment around three axes. Using these devices, reaction force from skin is calculated and analyzed.

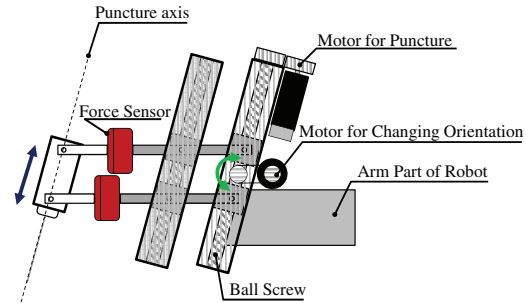


Fig. 5. End-effector of ZeroBot

### C. Procedure of Puncture

This subsection shows procedure of Robotic IR. The procedure is listed below.

- 1) CT radiography  
Target tumor's position is confirmed from patient's CT image.
- 2) Planning  
Relation between catheter marker and tumor position is confirmed by CT image, and puncture path is planned. Then, a puncturing point on surface of skin is marked.
- 3) Adjustment of Needle Tip Position and Needle Orientation  
Needle is brought to CT radiography plane based on laser emitted from CT equipment. And needle tip position is adjusted to marked position on surface of skin. Then, needle orientation is adjusted to preplanned angle too.
- 4) Fine Adjustment  
Needle orientation is made fine adjustments so as to direct a needle to the target tumor, under CT guidance. Artifact from needle can be regarded as extension line of needle.
- 5) Puncture  
Needle puncture is performed. When the depth of puncture reaches the preplanned value, relation between needle tip and target tumor position is confirmed by CT radiography. And then, either needle tip position or needle orientation is operated as necessary.

ZeroBot is operated in this procedure. If robot cannot manipulate needle accurately, the surgeon have to readjust

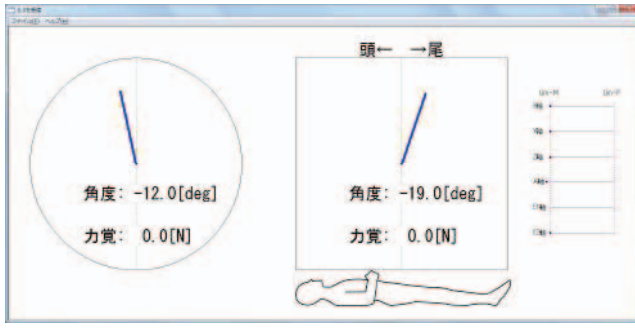


Fig. 6. Appearance of Navigation Display

the posture of needle based on real time CT image. It will cause increasing patient's radiation exposure. Therefore, accuracy of robot hand position is required.

#### D. Input Device

Design of input device is important because Zerobot is required operation by the doctor. Developed input device is shown in left side of Fig. 3. This interface consists from nine push buttons and a joystick. Right half of input panel, which is further on the right side than joystick, corresponds to actuate linear axis of X, Y and Z of Zerobot. On the other hand, left half of input panel which includes joystick corresponds to rotate around axis of X and Y, and to actuate axis of puncture. And speed of actuator is switchable so that needle puncture speed can be increased at the moment of penetrating surface of skin. Fig. 3 shows the input device is fixed on special stand. Also the device can be detached from the stand and can use from any position until wire stretch.

At the IR operation, needle orientation should be adjusted to the value decided at planning. But operator often cannot look at needle directly because Zerobot is remote controlled. Even if the needle could be sighted, fine adjustment of needle orientation is difficult. Therefore actual needle orientation should be shown intelligibly to operator. Then the navigation display which shows the needle orientation to operator by a picture was developed. The picture is shown in Fig. 6 on monitor of PC for controller. Two blue lines drawn in Fig. 6 indicates the needle orientation. There are two lines so that information of needle orientation on 3-D is divided into 2-D plane. A blue line drawn in the circle on left half of the picture corresponds the angle of the needle on the CT image. And right side one corresponds the angle of the needle on the plane, which includes needle and is located vertical from CT radiography plane (When this angle is zero, straight line which includes needle crosses with X axis vertically.). Operator can confirm the needle orientation, by looking the blue lines and displayed values of angle, in order to adjust the needle orientation to the preplanned angle.

### III. ANIMAL EXPERIMENT

In order to confirm the problem on conducting Robotic IR, puncture experiment is significant. CT-IR phantom[7] puncture experiment is conducted as dry run of Robotic IR. But reproducing deformation of needle caused by deflection or

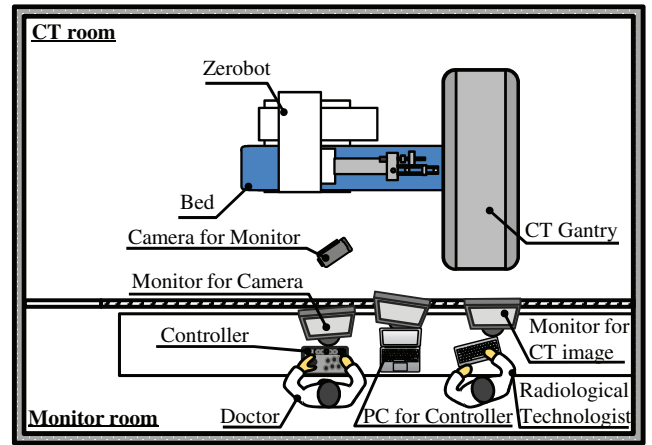


Fig. 7. Environment of Animal Experiment

softness of human skin is difficult. An effect on performance of Zerobot caused by deflection of skin and moving body tissue should be confirmed. Therefore animal experiment with rabbit was conducted.

#### A. Environment of Animal Experiment

This subsection shows the environment of animal experiment. The experiment conducted at Okayama Medical Innovation Center, Okayama University. Environment of the experiment is shown in Fig. 7. The rabbit is fixed on the bed, shaved body hair and scanned CT image. The doctor designated some rabbit's body tissues from CT image, and marked needle inserting point on the rabbit's skin. And then, puncture to the rabbit is performed following the procedure of subsection of II-C. Length of the needle which was used in this experiment is 75[mm], and diameter of the needle is 20 gauge (approx. 0.81[mm] diam.). Diameter of needle which includes needle guide is approximately 1.1[mm]. And the needle is made of stainless steel.

Mount of force sensors is shown in Fig. 8. Each sensor can measure the moment around axis of  $X_i$ ,  $Y_i$  and  $Z_i$  ( $i = 1, 2$ ). Using the moment values measured by two sensors, puncture reaction force is calculated. When  $F_x$ ,  $F_y$  and  $F_z$  are applied to the point of action,  $F_x$  effects to values of  $M_{yi}$  and  $M_{zi}$ . On the other hands,  $F_y$  and  $F_z$  effects to values of  $M_{xi}$ . So we can calculate the value of  $F_x$  from  $M_{yi}$  and  $M_{zi}$ . But  $F_y$  and  $F_z$  should be calculated from only value of  $M_{xi}$ , so we cannot determine these values uniquely. In order to calculate these values uniquely, we assume that the value of  $F_z$  is almost zero because needle can be confirmed on the CT image during puncture. Then equations (1) to (3) can be derivated.

$$F_z \approx 0, \quad (1)$$

$$F_x = \frac{M_{z1}}{l_2} + \frac{M_{z2}}{l_3} + \frac{1}{l_1} (M_{y1} + M_{y2}), \quad (2)$$

$$F_y = -\frac{1}{l_1} (M_{x1} + M_{x2}). \quad (3)$$

$F_y$  is puncture reaction force.  $F_x$  is direction of needle deflection. When needle deflects, we can calculate theoretical

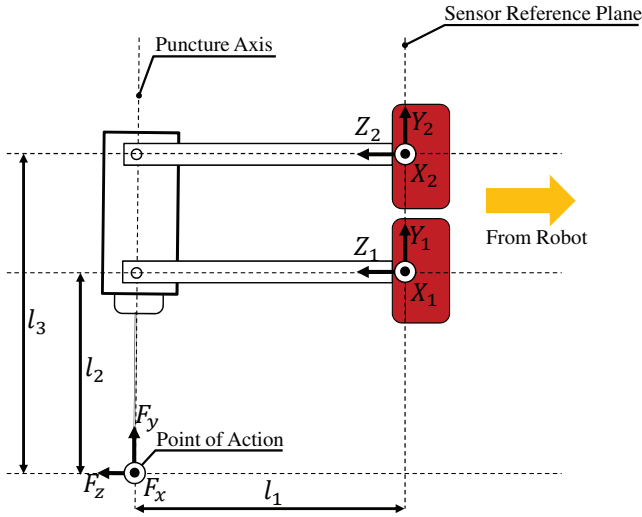


Fig. 8. Layout Drawing of Force Sensor

value of  $F_x$  from displacement based on equations (4, 5).

$$I = \frac{\pi d^4}{64}, \quad (4)$$

$$F_x^* = \frac{3EI\delta}{l_E^3}. \quad (5)$$

Here,  $F_x^*$  is the theoretical value of  $F_x$ ,  $l_E$  is the whole length of needle,  $E$  is the Young's modulus,  $I$  is second moment of area,  $d$  is diameter of needle includes needle guide and  $\delta$  is displacement of deflected needle tip. Parameters which are required in these equations (1) to (5) are shown in TABLE I.

Here, CT image of deflected needle in animal experiment is shown in Fig. 9. Displacement of deflected needle tip is 8.0[mm], which is measured on CT image (in the CT image, one pixel is approximately 0.4[mm]). Therefore the value of  $F_x^*$  is calculated as 0.8[N]. The graph of  $F_x$  measured by force sensors of this case is shown in Fig. 10. The value of  $F_x$  is approximately 0.9[N] when needle deflects in the graph. Comparing  $F_x$  value and  $F_x^*$  value, we can calculate proper  $F_x$  value by equation (2, 5).

## B. Result

Rabbit's body is tender than human's. But rabbit's surface skin is harder than human's skin. So needle cannot be inserted into rabbit via surface skin even if the doctor tries to insert needle by his hand. Therefore needle inserting point

which is marked at planning stage was incised epidermally. Experimental results are shown in Fig. 11 to Fig. 13.

Experimental results in the case of successful puncturing is shown in Fig. 11. It is confirmed that needle tip position has reached to target point at CT image shown in Fig. 11(a). Reaction force is shown in Fig. 11(b). It is confirmed that needle is inserted deeper,  $F_y$  varies rapidly. On the other hand, the value of  $F_x$  is almost constant. In this case, considering from these facts, reaction force was applied to only direction of puncture axis. Fig. 11(c) shows the relationship between reaction force and depth of puncture between  $A_1$  and  $B_1$ . As the needle goes forward to forward,  $F_y$  value increases linearly. Therefore surface skin of rabbit's body tissue has spring property. But after depth of puncture reaches to  $C_1$ , the spring property is broken because surface skin succumbs to puncture force. We can conjecture that destruction of spring property is caused by needle penetration.

Fig. 12 shows experimental result, under the condition path plan of needle goes through issue close to bone. In this case, trajectory of needle insertion was affected by deflection of needle. This fact is confirmed from Fig. 12(a). In Fig. 12(b), it is confirmed that  $F_x$  finally reaches approximately 1[N]. We can conjecture that the increase of  $F_x$  is caused by needle deflection. Fig. 12(c) shows the force between  $A_2$  and  $B_2$  in a same way of Fig. 11(c). The spring property is shown until depth of puncture reaches  $C_2$ , and after that, the spring property is broken. Comparing Fig. 11(c) and Fig. 12(c), absolute ratio of  $F_x$  to  $F_y$  in the latter graph is larger than that in former.

Failed puncture data is shown in Fig. 13. In this case, puncture was failure because the needle inserting point of rabbit's surface skin is not performed skin incision. Deflection of surface skin and needle is confirmed from Fig. 13(a). In the graph of reaction force shown in Fig. 13(b), transition

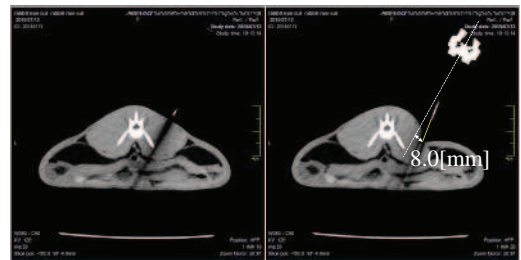


Fig. 9. CT Image of Deflected Needle

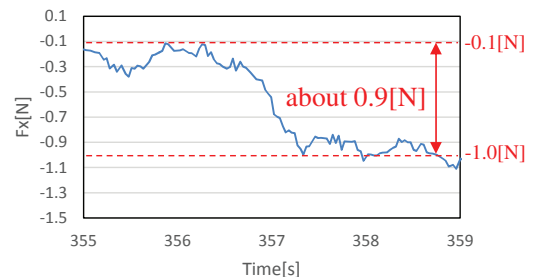
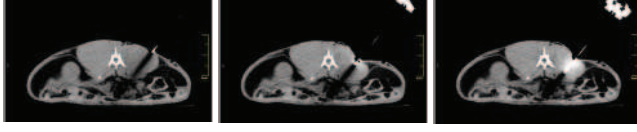


Fig. 10.  $F_x$  in the Case of Deflecting Needle

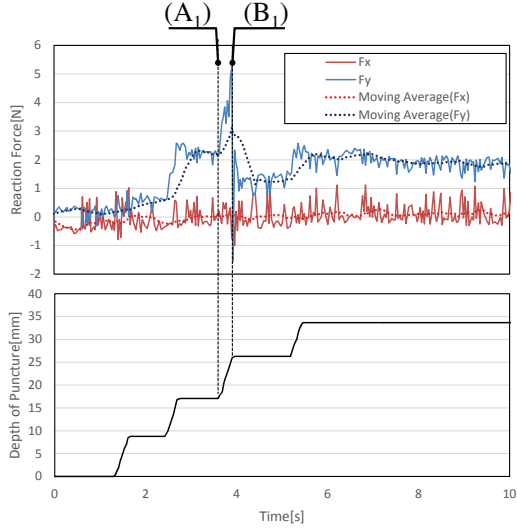
TABLE I  
PARAMETERS FOR CALCULATION OF FORCE VALUES

Parameter	Value
$l_1$	0.118[m]
$l_2$	0.0811[m]
$l_3$	0.14[m]
$l_E$	0.0075[m]
$d$	0.0011[m]
$E$	200000[MPa]

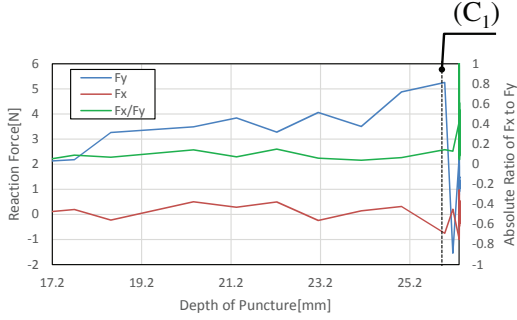




(a)



(b)

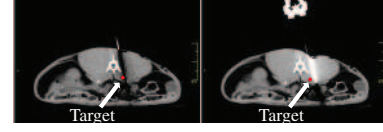


(c)

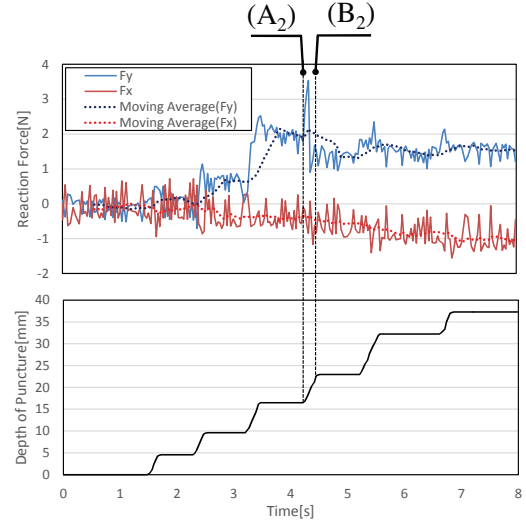
Fig. 11. Experimental data of puncture far from bone. (a) is CT image, (b) is reaction force and depth of puncture, and (c) is relationship between reaction force and depth of puncture. In (c), the horizontal axis shows depth of puncture, the vertical axis of the left side shows the value of reaction force, and the right side one shows the absolute ratio of  $F_x$  to  $F_y$ .

of  $F_x$  and  $F_y$  shows the almost same shape. And in Fig. 13(c), destruction of spring property is not shown and absolute ratio of  $F_x$  to  $F_y$  is almost 1.

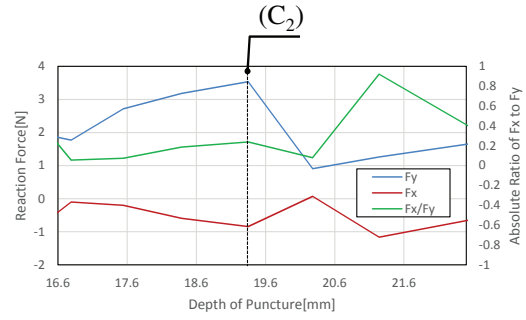
We assume the model of rabbit's tissue as shown in Fig. 14(a). If needle penetrates rabbit's skin, needle is constrained by spring property of rabbit's body tissue. When deflection force applies to needle in this case, spring property prevents the force increasing because needle tip displaces. Therefore inclination of  $F_x$  cannot increase rapidly. Next, we derived the failed puncture model as shown in Fig. 14(b). In this figure,  $\Delta Y$  means the velocity of puncture. When



(a)



(b)



(c)

Fig. 12. Experimental data of puncture close to bone. (a) is CT image, (b) is reaction force and depth of puncture, and (c) is relationship between reaction force and depth of puncture. In (c), the horizontal axis shows depth of puncture, the vertical axis of the left side shows the value of reaction force, and the right side one shows the absolute ratio of  $F_x$  to  $F_y$ .

puncture failed, needle deflection is performed as a certain obstacle prevents the trajectory of needle. Therefore needle is punctured deeper, deflection force applies to more near point of needle's root. In this case, considering with equation (5),  $\delta$  is constant and  $l_E$  decreases linearly if  $\Delta Y$  is constant. So absolute value of  $F_x$  increases on the order of  $x^{-3}$ . Then we conjecture that  $F_x$  varies more rapidly in the case of failed than the case of penetrating. After that, we focused the inclination of  $F_x$  which is shown in Fig. 15. Inclination value of failed puncture reaches only under -0.5. In these cases, if we set threshold value to -0.5, it can be detected

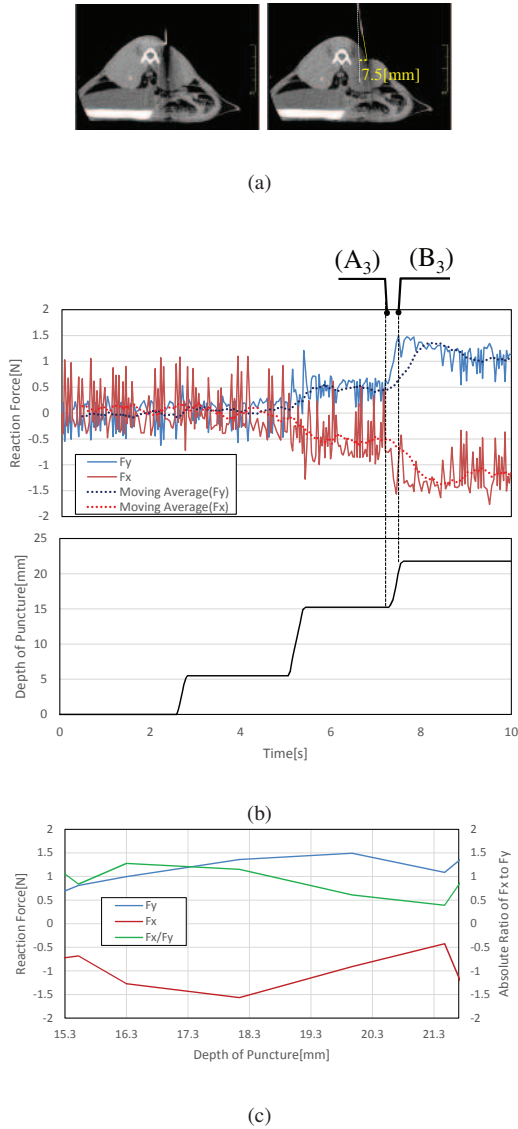


Fig. 13. Experimental data of failed puncture. (a) is CT image, (b) is reaction force and depth of puncture, and (c) is relationship between reaction force and depth of puncture. In (c), the horizontal axis shows depth of puncture, the vertical axis of the left side shows the value of reaction force, and the right side one shows the absolute ratio of  $F_x$  to  $F_y$ .

whether needle is punctured successfully or not.

#### IV. CONCLUSION

In this paper, overview of Robotic IR and animal puncture experiment are described. Zerobot has succeeded to insert needle to rabbit's body tissue. When needle is inserted to rabbit, deflection of needle caused by softness of rabbit's body tissue occurs. And trajectory of needle is affected by this problem. We can conjecture that this problem occurs also at the time of inserting needle to human.

When a needle penetrate surface skin, destruction of spring property of skin was confirmed. In order to detect deflection of needle,  $F_x$  value is significant. If inclination of  $F_x$  value was over some threshold, it is expected that the system can

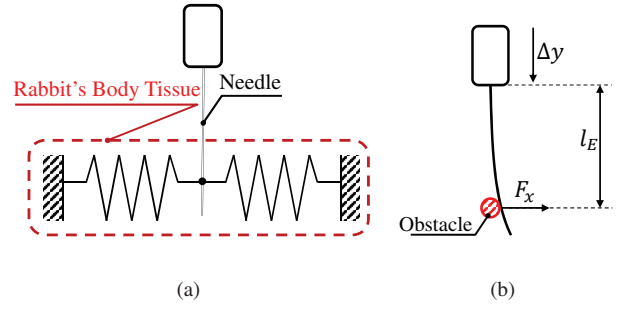


Fig. 14. (a) Model of rabbit's body tissue and (b) model of failed puncture.

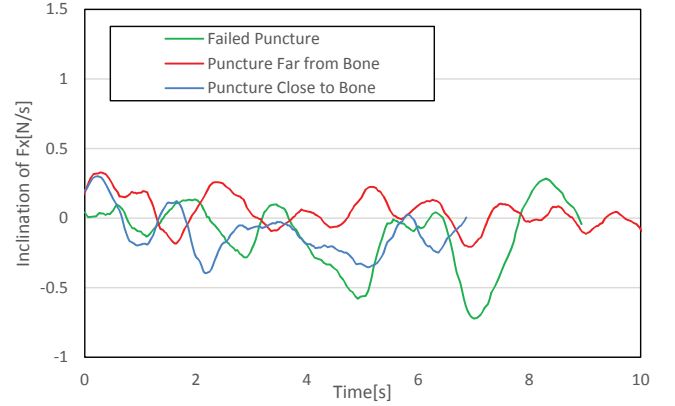


Fig. 15. Inclination of  $F_x$ . In this graph,  $F_x$  values in the all cases applied moving average filter because these values include high-frequency noise. After the filter applies, inclination of approximation straight line of 30 vicinity value is plotted.

detect failure of inserting needle.

#### REFERENCES

- [1] Japan IR Society, "http://www.jsivr.jp/"
- [2] Takao Hiraki, Tetsushi Kamegawa, Takayuki Matsuno, Susumu Kanazawa, "Development of a Robot for CT Fluoroscopy-guided Intervention : Free Physicians from Radiation", *Jon J Intervent Radiol*, 20:375-381, 2014.
- [3] Takao Hiraki, Hideo Gohara, Hidefumi Mimura, Shinichi Toyooka, Hiroyasu Fujiwara, Kotaro Yasui, Yoshifumi Sano, Toshihiro Iguchi, Jun Sakurai, Nobuhisa Tajiri, Takashi Mukai, Yusuke Matsui, Susumu Kanazawa, "Radiofrequency Ablation of Lung Cancer at Okayama University Hospital: A Review of 10 Years of Experience", *Acta Med.*, Vol.65, No.5, pp. 287-297, Okayama, 2011.
- [4] Dan Staiianovici, Kevin Cleary, Alexandru Patriciu, Dumitru Mazilu, Alexandru Stanimir, Nicolae Craciunoiu, Vance Watson, Louis Kavoussi, "AcuBot: A Robot for Radiological Interventions", *IEEE TRANSACTIONS ON ROBOTICS AND AUTOMATION*, VOL.19, NO.5, pp.927-930, OCTOBER 2003.
- [5] Benjamin Maurin, Bernard Bayle, Olivier Piccin, Jacques Gangloff, Michel de Mathelin, Christophe Doignon, Philippe Zanne, Afshin Gangi, "A Patient-Mounted Robotic Platform for CT-Scan Guided Procedures", *IEEE TRANSACTIONS ON BIOMEDICAL ENGINEERING*, VOL.55, NO.10, OCTOBER, 2008.
- [6] Joachim Kettenbach, Gernot Kronreif, Michael Figl, Martin Fürst, Wolfgang Birkfellner, Rudolf Hanel, Wolfgang Ptacek, Helmar Bergmann, "Robot-Assisted Biopsy Using Computed Tomography-Guidance Initial Results From In Vitro Tests", *Investigative Radiology*, Volume 40, Number 4, pp.219-228, April 2005.
- [7] Hirotaka Nakaya, Takayuki Matsuno, Tetsushi Kamegawa, Takao Hiraki, Takuya Inoue, Mamoru Minami, Akira Yanou, Akio Gofuku, "Development and Evaluation of Phantom for CT-IVR", *JSME Conference on Robotics and Mechatronics*, Toyama, Japan, 2014.